Search for Diphoton Events with Large Missing Transverse Energy in 6.3 fb^{-1} of $p\bar{p}$ Collisions at $\sqrt{s} = 1.96$ TeV

V. M. Abazov,[35] B. Abbott,[73] M. Abolins,[62] B. S. Acharya,[29] M. Adams,[48] T. Adams,[46] G. D. Alexeev,[35] G. Alkhazov,[39] A. Alton,[61,*] G. Alverson,[60] G. A. Alves,[2] L. S. Ancu,[34] M. Aoki,[47] Y. Arnoud,[14] M. Arov,[57] A. Askew,[46] B. Åsman,[40] O. Atramentov,[65] C. Avila,[8] J. BackusMayes,[80] F. Badaud,[13] L. Bagby,[47] B. Baldin,[47] D. V. Bandurin,[46] S. Banerjee,[29] E. Barberis,[60] P. Baringer,[55] J. Barreto,[2] J. F. Bartlett,[47] U. Bassler,[18] S. Beale,[6] A. Bean,[55] M. Begalli,[3] M. Begel,[71] C. Belanger-Champagne,[40] L. Bellantoni,[47] J. A. Benitez,[62] S. B. Beri,[27] G. Bernardi,[17] R. Bernhard,[22] I. Bertram,[41] M. Besançon,[18] R. Beuselinck,[42] V. A. Bezzubov,[38] P. C. Bhat,[47] V. Bhatnagar,[27] G. Blazey,[49] S. Blessing,[46] K. Bloom,[64] A. Boehnlein,[47] D. Boline,[70] T. A. Bolton,[56] E. E. Boos,[37] G. Borissov,[41] T. Bose,[59] A. Brandt,[76] O. Brandt,[23] R. Brock,[62] G. Brooijmans,[68] A. Bross,[47] D. Brown,[17] J. Brown,[17] X. B. Bu,[7] D. Buchholz,[50] M. Buehler,[79] V. Buescher,[24] V. Bunichev,[37] S. Burdin,[41,†] T. H. Burnett,[80] C. P. Buszello,[42] B. Calpas,[15] S. Calvet,[16] E. Camacho-Pérez,[32] M. A. Carrasco-Lizarraga,[32] E. Carrera,[46] B. C. K. Casey,[47] H. Castilla-Valdez,[32] S. Chakrabarti,[70] D. Chakraborty,[49] K. M. Chan,[53] A. Chandra,[78] G. Chen,[55] S. Chevalier-Théry,[18] D. K. Cho,[75] S. W. Cho,[31] S. Choi,[31] B. Choudhary,[28] T. Christoudias,[42] S. Cihangir,[47] D. Claes,[64] J. Clutter,[55] M. S. Cooke,[68] M. Cooke,[47] W. E. Cooper,[47] M. Corcoran,[78] F. Couderc,[18] M.-C. Cousinou,[15] A. Croc,[18] D. Cutts,[75] M. Ćwiok,[30] A. Das,[44] G. Davies,[42] K. De,[76] S. J. de Jong,[34] E. De La Cruz-Burelo,[32] F. Déliot,[18] M. Demarteau,[47] R. Demina,[69] D. Denisov,[47] S. P. Denisov,[38] S. Desai,[47] K. DeVaughan,[64] H. T. Diehl,[47] M. Diesburg,[47] A. Dominguez,[64] T. Dorland,[80] A. Dubey,[28] L. V. Dudko,[37] D. Duggan,[65] A. Duperrin,[15] S. Dutt,[27] A. Dyshkant,[49] M. Eads,[64] D. Edmunds,[62] J. Ellison,[45] V. D. Elvira,[47] Y. Enari,[17] S. Eno,[58] H. Evans,[51] A. Evdokimov,[71] V. N. Evdokimov,[38] G. Facini,[60] A. V. Ferapontov,[75] T. Ferbel,[58,69] F. Fiedler,[24] F. Filthaut,[34] W. Fisher,[62] H. E. Fisk,[47] M. Fortner,[49] H. Fox,[41] S. Fuess,[47] T. Gadfort,[71] A. Garcia-Bellido,[69] V. Gavrilov,[36] P. Gay,[13] W. Geist,[19] W. Geng,[15,62] D. Gerbaudo,[66] C. E. Gerber,[48] Y. Gershtein,[65] G. Ginther,[47,69] G. Golovanov,[35] A. Goussiou,[80] P. D. Grannis,[70] S. Greder,[19] H. Greenlee,[47] Z. D. Greenwood,[57] E. M. Gregores,[4] G. Grenier,[20] Ph. Gris,[13] J.-F. Grivaz,[16] A. Grohsjean,[18] S. Grünendahl,[47] M. W. Grünewald,[30] F. Guo,[70] J. Guo,[70] G. Gutierrez,[47] P. Gutierrez,[73] A. Haas,[68,‡] S. Hagopian,[46] J. Haley,[60] L. Han,[7] K. Harder,[43] A. Harel,[69] J. M. Hauptman,[54] J. Hays,[42] T. Hebbeker,[21] D. Hedin,[49] H. Hegab,[74] A. P. Heinson,[45] U. Heintz,[75] C. Hensel,[23] I. Heredia-De La Cruz,[32] K. Herner,[61] G. Hesketh,[60] M. D. Hildreth,[53] R. Hirosky,[79] T. Hoang,[46] J. D. Hobbs,[70] B. Hoeneisen,[12] M. Hohlfeld,[24] S. Hossain,[73] Z. Hubacek,[10] N. Huske,[17] V. Hynek,[10] I. Iashvili,[67] R. Illingworth,[47] A. S. Ito,[47] S. Jabeen,[75] M. Jaffré,[16] S. Jain,[67] D. Jamin,[15] R. Jesik,[42] K. Johns,[44] M. Johnson,[47] D. Johnston,[64] A. Jonckheere,[47] P. Jonsson,[42] J. Joshi,[27] A. Juste,[47,§] K. Kaadze,[56] E. Kajfasz,[15] D. Karmanov,[37] P. A. Kasper,[47] I. Katsanos,[64] R. Kehoe,[77] S. Kermiche,[15] N. Khalatyan,[47] A. Khanov,[74] A. Kharchilava,[67] Y. N. Kharzheev,[35] D. Khatidze,[75] M. H. Kirby,[50] J. M. Kohli,[27] A. V. Kozelov,[38] J. Kraus,[62] A. Kumar,[67] A. Kupco,[11] T. Kurča,[20] V. A. Kuzmin,[37] J. Kvita,[9] S. Lammers,[51] G. Landsberg,[75] P. Lebrun,[20] H. S. Lee,[31] S. W. Lee,[54] W. M. Lee,[47] J. Lellouch,[17] L. Li,[45] Q. Z. Li,[47] S. M. Lietti,[5] J. K. Lim,[31] D. Lincoln,[47] J. Linnemann,[62] V. V. Lipaev,[38] R. Lipton,[47] Y. Liu,[7] Z. Liu,[6] A. Lobodenko,[39] M. Lokajicek,[11] P. Love,[41] H. J. Lubatti,[80] R. Luna-Garcia,[32,‖] A. L. Lyon,[47] A. K. A. Maciel,[2] D. Mackin,[78] R. Madar,[18] R. Magaña-Villalba,[32] S. Malik,[64] V. L. Malyshev,[35] Y. Maravin,[56] J. Martínez-Ortega,[32] R. McCarthy,[70] C. L. McGivern,[55] M. M. Meijer,[34] A. Melnitchouk,[63] D. Menezes,[49] P. G. Mercadante,[4] M. Merkin,[37] A. Meyer,[21] J. Meyer,[23] N. K. Mondal,[29] G. S. Muanza,[15] M. Mulhearn,[79] E. Nagy,[15] M. Naimuddin,[28] M. Narain,[75] R. Nayyar,[28] H. A. Neal,[61] J. P. Negret,[8] P. Neustroev,[39] H. Nilsen,[22] S. F. Novaes,[5] T. Nunnemann,[25] G. Obrant,[39] D. Onoprienko,[56] J. Orduna,[32] N. Osman,[42] J. Osta,[53] G. J. Otero y Garzón,[1] M. Owen,[43] M. Padilla,[45] M. Pangilinan,[75] N. Parashar,[52] V. Parihar,[75] S. K. Park,[31] J. Parsons,[68] R. Partridge,[75,‡] N. Parua,[51] A. Patwa,[71] B. Penning,[47] M. Perfilov,[37] K. Peters,[43] Y. Peters,[43] G. Petrillo,[69] P. Pétroff,[16] R. Piegaia,[1] J. Piper,[62] M.-A. Pleier,[71] P. L. M. Podesta-Lerma,[32,¶] V. M. Podstavkov,[47] M.-E. Pol,[2] P. Polozov,[36] A. V. Popov,[38] M. Prewitt,[78] D. Price,[51] S. Protopopescu,[71] J. Qian,[61] A. Quadt,[23] B. Quinn,[63] M. S. Rangel,[16] K. Ranjan,[28] P. N. Ratoff,[41] I. Razumov,[38] P. Renkel,[77] P. Rich,[43] M. Rijssenbeek,[70] I. Ripp-Baudot,[19] F. Rizatdinova,[74] M. Rominsky,[47] C. Royon,[18] P. Rubinov,[47] R. Ruchti,[53] G. Safronov,[36] G. Sajot,[14] A. Sánchez-Hernández,[32] M. P. Sanders,[25] B. Sanghi,[47] A. S. Santos,[5] G. Savage,[47] L. Sawyer,[57] T. Scanlon,[42] R. D. Schamberger,[70] Y. Scheglov,[39] H. Schellman,[50] T. Schliephake,[26] S. Schlobohm,[80] C. Schwanenberger,[43] R. Schwienhorst,[62] J. Sekaric,[55] H. Severini,[73] E. Shabalina,[23] V. Shary,[18] A. A. Shchukin,[38] R. K. Shivpuri,[28] V. Simak,[10] V. Sirotenko,[47] P. Skubic,[73] P. Slattery,[69] D. Smirnov,[53] K. J. Smith,[67] G. R. Snow,[64] J. Snow,[72] S. Snyder,[71] S. Söldner-Rembold,[43] L. Sonnenschein,[21] A. Sopczak,[41] M. Sosebee,[76] K. Soustruznik,[9] B. Spurlock,[76] J. Stark,[14] V. Stolin,[36] D. A. Stoyanova,[38] E. Strauss,[70] M. Strauss,[73] D. Strom,[48] L. Stutte,[47] P. Svoisky,[34]

M. Takahashi,[43] A. Tanasijczuk,[1] W. Taylor,[6] M. Titov,[18] V. V. Tokmenin,[35] D. Tsybychev,[70] B. Tuchming,[18] C. Tully,[66] P. M. Tuts,[68] L. Uvarov,[39] S. Uvarov,[39] S. Uzunyan,[49] R. Van Kooten,[51] W. M. van Leeuwen,[33] N. Varelas,[48] E. W. Varnes,[44] I. A. Vasilyev,[38] P. Verdier,[20] L. S. Vertogradov,[35] M. Verzocchi,[47] M. Vesterinen,[43] D. Vilanova,[18] P. Vint,[42] P. Vokac,[10] H. D. Wahl,[46] M. H. L. S. Wang,[69] J. Warchol,[53] G. Watts,[80] M. Wayne,[53] M. Weber,[47,**] M. Wetstein,[58] A. White,[76] D. Wicke,[24] M. R. J. Williams,[41] G. W. Wilson,[55] S. J. Wimpenny,[45] M. Wobisch,[57] D. R. Wood,[60] T. R. Wyatt,[43] Y. Xie,[47] C. Xu,[61] S. Yacoob,[50] R. Yamada,[47] W.-C. Yang,[43] T. Yasuda,[47] Y. A. Yatsunenko,[35] Z. Ye,[47] H. Yin,[7] K. Yip,[71] H. D. Yoo,[75] S. W. Youn,[47] J. Yu,[76] S. Zelitch,[79] T. Zhao,[80] B. Zhou,[61] N. Zhou,[68] J. Zhu,[61] M. Zielinski,[69] D. Zieminska,[51] and L. Zivkovic[68]

(D0 Collaboration)

[1]*Universidad de Buenos Aires, Buenos Aires, Argentina*
[2]*LAFEX, Centro Brasileiro de Pesquisas Físicas, Rio de Janeiro, Brazil*
[3]*Universidade do Estado do Rio de Janeiro, Rio de Janeiro, Brazil*
[4]*Universidade Federal do ABC, Santo André, Brazil*
[5]*Instituto de Física Teórica, Universidade Estadual Paulista, São Paulo, Brazil*
[6]*Simon Fraser University, Vancouver, British Columbia, Canada, and York University, Toronto, Ontario, Canada*
[7]*University of Science and Technology of China, Hefei, People's Republic of China*
[8]*Universidad de los Andes, Bogotá, Colombia*
[9]*Charles University, Faculty of Mathematics and Physics, Center for Particle Physics, Prague, Czech Republic*
[10]*Czech Technical University in Prague, Prague, Czech Republic*
[11]*Center for Particle Physics, Institute of Physics, Academy of Sciences of the Czech Republic, Prague, Czech Republic*
[12]*Universidad San Francisco de Quito, Quito, Ecuador*
[13]*LPC, Université Blaise Pascal, CNRS/IN2P3, Clermont, France*
[14]*LPSC, Université Joseph Fourier Grenoble 1, CNRS/IN2P3, Institut National Polytechnique de Grenoble, Grenoble, France*
[15]*CPPM, Aix-Marseille Université, CNRS/IN2P3, Marseille, France*
[16]*LAL, Université Paris-Sud, CNRS/IN2P3, Orsay, France*
[17]*LPNHE, Universités Paris VI and VII, CNRS/IN2P3, Paris, France*
[18]*CEA, Irfu, SPP, Saclay, France*
[19]*IPHC, Université de Strasbourg, CNRS/IN2P3, Strasbourg, France*
[20]*IPNL, Université Lyon 1, CNRS/IN2P3, Villeurbanne, France and Université de Lyon, Lyon, France*
[21]*III. Physikalisches Institut A, RWTH Aachen University, Aachen, Germany*
[22]*Physikalisches Institut, Universität Freiburg, Freiburg, Germany*
[23]*II. Physikalisches Institut, Georg-August-Universität Göttingen, Göttingen, Germany*
[24]*Institut für Physik, Universität Mainz, Mainz, Germany*
[25]*Ludwig-Maximilians-Universität München, München, Germany*
[26]*Fachbereich Physik, Bergische Universität Wuppertal, Wuppertal, Germany*
[27]*Panjab University, Chandigarh, India*
[28]*Delhi University, Delhi, India*
[29]*Tata Institute of Fundamental Research, Mumbai, India*
[30]*University College Dublin, Dublin, Ireland*
[31]*Korea Detector Laboratory, Korea University, Seoul, Korea*
[32]*CINVESTAV, Mexico City, Mexico*
[33]*FOM-Institute NIKHEF and University of Amsterdam/NIKHEF, Amsterdam, The Netherlands*
[34]*Radboud University Nijmegen/NIKHEF, Nijmegen, The Netherlands*
[35]*Joint Institute for Nuclear Research, Dubna, Russia*
[36]*Institute for Theoretical and Experimental Physics, Moscow, Russia*
[37]*Moscow State University, Moscow, Russia*
[38]*Institute for High Energy Physics, Protvino, Russia*
[39]*Petersburg Nuclear Physics Institute, St. Petersburg, Russia*
[40]*Stockholm University, Stockholm and Uppsala University, Uppsala, Sweden*
[41]*Lancaster University, Lancaster LA1 4YB, United Kingdom*
[42]*Imperial College London, London SW7 2AZ, United Kingdom*
[43]*The University of Manchester, Manchester M13 9PL, United Kingdom*
[44]*University of Arizona, Tucson, Arizona 85721, USA*
[45]*University of California Riverside, Riverside, California 92521, USA*
[46]*Florida State University, Tallahassee, Florida 32306, USA*
[47]*Fermi National Accelerator Laboratory, Batavia, Illinois 60510, USA*
[48]*University of Illinois at Chicago, Chicago, Illinois 60607, USA*

[49]Northern Illinois University, DeKalb, Illinois 60115, USA
[50]Northwestern University, Evanston, Illinois 60208, USA
[51]Indiana University, Bloomington, Indiana 47405, USA
[52]Purdue University Calumet, Hammond, Indiana 46323, USA
[53]University of Notre Dame, Notre Dame, Indiana 46556, USA
[54]Iowa State University, Ames, Iowa 50011, USA
[55]University of Kansas, Lawrence, Kansas 66045, USA
[56]Kansas State University, Manhattan, Kansas 66506, USA
[57]Louisiana Tech University, Ruston, Louisiana 71272, USA
[58]University of Maryland, College Park, Maryland 20742, USA
[59]Boston University, Boston, Massachusetts 02215, USA
[60]Northeastern University, Boston, Massachusetts 02115, USA
[61]University of Michigan, Ann Arbor, Michigan 48109, USA
[62]Michigan State University, East Lansing, Michigan 48824, USA
[63]University of Mississippi, University, Mississippi 38677, USA
[64]University of Nebraska, Lincoln, Nebraska 68588, USA
[65]Rutgers University, Piscataway, New Jersey 08855, USA
[66]Princeton University, Princeton, New Jersey 08544, USA
[67]State University of New York, Buffalo, New York 14260, USA
[68]Columbia University, New York, New York 10027, USA
[69]University of Rochester, Rochester, New York 14627, USA
[70]State University of New York, Stony Brook, New York 11794, USA
[71]Brookhaven National Laboratory, Upton, New York 11973, USA
[72]Langston University, Langston, Oklahoma 73050, USA
[73]University of Oklahoma, Norman, Oklahoma 73019, USA
[74]Oklahoma State University, Stillwater, Oklahoma 74078, USA
[75]Brown University, Providence, Rhode Island 02912, USA
[76]University of Texas, Arlington, Texas 76019, USA
[77]Southern Methodist University, Dallas, Texas 75275, USA
[78]Rice University, Houston, Texas 77005, USA
[79]University of Virginia, Charlottesville, Virginia 22901, USA
[80]University of Washington, Seattle, Washington 98195, USA

(Received 14 August 2010; published 24 November 2010)

We report a search for diphoton events with large missing transverse energy produced in $p\bar{p}$ collisions at $\sqrt{s} = 1.96$ TeV. The data were collected with the D0 detector at the Fermilab Tevatron Collider and correspond to 6.3 fb^{-1} of integrated luminosity. The observed missing transverse energy distribution is well described by the standard model prediction, and 95% C.L. limits are derived on two realizations of theories beyond the standard model. In a gauge-mediated supersymmetry breaking scenario, the breaking scale Λ is excluded for $\Lambda < 124$ TeV. In a universal extra dimension model including gravitational decays, the compactification radius R_c is excluded for $R_c^{-1} < 477$ GeV.

DOI: 10.1103/PhysRevLett.105.221802 PACS numbers: 14.80.Ly, 12.60.Jv, 13.85.Rm, 14.80.Rt

In the standard model (SM), events with two high transverse momentum photons ($\gamma\gamma$) and large missing transverse energy [1] ($\not\!\!E_T$) are produced at a small rate in $p\bar{p}$ collisions. This final state is therefore sensitive to contributions from processes beyond the SM (BSM). We report a search for $\gamma\gamma$ events with large $\not\!\!E_T$ produced in $p\bar{p}$ collisions recorded by using the D0 detector at the Fermilab Tevatron Collider. The sensitivity is assessed for two benchmark BSM models, gauge-mediated supersymmetry (SUSY) breaking (GMSB) [2] and universal extra dimensions (UED) [3].

In GMSB models, the masses of the SUSY partners to SM particles arise from SM gauge interactions and are proportional to the effective SUSY breaking scale Λ. As the gravitino ($\tilde{G}$) does not participate in SM gauge interactions, it has a small mass [4] and is the lightest SUSY particle. Assuming R parity conservation [5], the SUSY process with the largest cross section at the Tevatron would be chargino and neutralino pair production ($\chi_1^{\pm}\chi_2^0$, $\chi_1^{\pm}\chi_1^{\mp}$) [6], followed by decay chains to the next-to-lightest SUSY particle. We consider the case when the lightest neutralino (χ_1^0) is the next-to-lightest SUSY particle [7] and decays promptly with the dominant branching fraction yielding a photon and an essentially massless gravitino ($\chi_1^0 \rightarrow \tilde{G}\gamma$) [8]. The two gravitinos escape detection, resulting in the final state $\gamma\gamma + \not\!\!E_T + X$, where X denotes leptons and jets produced in the decay chains [9].

In UED models, extra spatial dimensions are predicted that are accessible to all SM fields. We consider the case of a single UED that is compactified with radius R_c, resulting

in a tower of states for each SM field, called Kaluza-Klein (KK) excitations, with the masses of these states separated by R_c^{-1}. At the Tevatron, the UED process with the largest cross section would be the production of pairs of first-level KK quarks [10], followed by decay chains to the lightest KK particle, the KK photon (γ^*). If additional larger extra dimensions also exist that are only accessible to gravity, the lightest KK particle is able to decay promptly through gravitational interactions to a photon and a graviton ($\gamma^* \rightarrow G\gamma$) [11,12]. The two gravitons escape detection, resulting in the final state $\gamma\gamma + \not{E}_T + X$.

Searches for BSM physics in $\gamma\gamma + \not{E}_T + X$ events have been performed at the CERN e^+e^- Collider (LEP) [13] and at the Tevatron in run I [14] and run II [15–18]. This analysis uses similar search methods to those adopted in Ref. [18] and employs a 6 times larger data set and improved photon identification criteria utilizing a neural network (NN) discriminant. The photon NN discriminant has been recently used in a measurement [19] by D0 of differential cross sections and kinematic properties of $\gamma\gamma$ events produced at the Tevatron. The larger data set has substantially increased the search sensitivity and has allowed an improved formulation of the data-derived SM background prediction. The background prediction, including the assessment of systematic uncertainties, was developed by using only the $\not{E}_T \leq 50$ GeV region of the $\gamma\gamma$ sample. Once finalized, the events with $\not{E}_T > 50$ GeV were included in evaluating the consistency with the SM prediction and the sensitivity to the signal models. In addition to substantially improved limits on the GMSB model, this Letter also presents the first limits on the UED model with gravitational decays.

The D0 detector [20] consists of an inner tracker, a liquid-argon–uranium calorimeter, and a muon spectrometer. The tracking system is comprised of a silicon microstrip tracker and a central fiber tracker, both located within a 2 T superconducting solenoidal magnet. A central calorimeter covers pseudorapidities $|\eta| < 1.1$, and two end-cap calorimeters extend the coverage to $|\eta| < 4.2$, where $\eta = -\ln[\tan(\theta/2)]$, and θ is the polar angle with respect to the proton beam direction. The electromagnetic (EM) section of the calorimeter is segmented in four longitudinal layers (EM_i, $i = 1, 4$) with transverse segmentation $\Delta\eta \times \Delta\phi = 0.1 \times 0.1$ (ϕ is the azimuthal angle), except in EM3 where it is 0.05×0.05. A central preshower detector utilizing several layers of scintillating strips, positioned between the solenoid coil and central calorimeter, provides a precise measurement of EM shower position. The trajectory of photon candidates is reconstructed by combining the four EM-layer and central preshower detector measurements [18].

The data analyzed correspond to an integrated luminosity of 6.3 ± 0.4 fb^{-1} [21] and were selected by using a collection of EM calorimeter-based single electron and photon triggers that are close to 100% efficient for signal events from the benchmark models satisfying the acceptance requirements of this analysis. Events containing identified calorimeter noise patterns which could bias the $\not{E}_T$ distribution are removed. Diphoton candidate events are selected by requiring at least two photon candidates with transverse energy $E_T > 25$ GeV identified in the central calorimeter. Photon candidates are selected from EM clusters reconstructed within a cone of radius $\mathcal{R} \equiv \sqrt{(\Delta\eta)^2 + (\Delta\phi)^2} = 0.2$ by requiring (i) $\geq 95\%$ of the cluster energy be deposited in the EM layers, (ii) the calorimeter isolation variable $I \equiv [E_{\mathrm{tot}}(0.4) - E_{\mathrm{EM}}(0.2)]/E_{\mathrm{EM}}(0.2)$ be less than 0.10, where $E_{\mathrm{tot}}(\mathcal{R})$ [$E_{\mathrm{EM}}(\mathcal{R})$] is the total [EM] energy in a cone of radius $\mathcal{R}$ about the cluster centroid, (iii) the shower width in EM3 be consistent with an EM shower, (iv) the scalar sum of the transverse momentum (p_T) of tracks originating from the $p\bar{p}$ collision vertex (PV) in a $0.05 < \mathcal{R} < 0.4$ annulus about the cluster centroid be less than 2 GeV, and (v) the cluster not be spatially matched to a reconstructed track or a significant density of silicon microstrip tracker and central fiber tracker hits [18]. Further rejection of jets misidentified as photons is achieved with a requirement on the NN discriminant, which is trained by using a set of track, central preshower detector, and calorimeter-based variables [19]. The NN requirement is $\approx 98\%$ efficient for real photons and rejects $\approx 50\%$ of those jets that pass all other photon selection criteria.

Electrons satisfy the same requirements as photons, with the exception of the track veto [item (v)]. Jets are reconstructed with the iterative midpoint algorithm [22] with cone size $\mathcal{R} = 0.5$. The $\not{E}_T$ is determined by using calorimeter energy depositions with $|\eta| < 4.2$. Corrections are applied to $\not{E}_T$ to calibrate energy from EM objects and jets and to account for the p_T of muons. There are, in general, several $p\bar{p}$ interactions per crossing of the beams. The correct PV is identified in $\approx 98\%$ of signal model events. The photon trajectories must indicate that the candidates originate at the PV. This requirement ensures an accurate calculation of transverse energy in background events in which the correct PV is less efficiently identified and suppresses noncollision events, such as beam halo and cosmic rays, to a negligible level. The requirement is measured to be $\approx 86\%$ efficient for signal model events using a $Z(\rightarrow ee, \mu\mu) + \gamma$ data sample. To reduce the number of events with significantly mismeasured $\not{E}_T$, events are rejected if the difference in azimuthal angle ($\Delta\phi$) between either photon and $\not{E}_T$ is less than 0.2 rad, or if $\Delta\phi$ between the highest E_T jet (if present) and $\not{E}_T$ is greater than 2.5 rad. No explicit requirement is made on the presence of jets and leptons in the event. A total of 7934 $\gamma\gamma$ candidate events satisfy the selection criteria.

SM background events in the $\gamma\gamma$ sample are categorized as arising from instrumental $\not{E}_T$ sources (SM $\gamma\gamma$, γ + jet, multijet) and genuine $\not{E}_T$ sources ($W\gamma$, W + jet, $W/Z + \gamma\gamma$). All backgrounds are measured by using data control

samples, with the exception of small contributions from $W/Z + \gamma\gamma$ events, which are estimated by using Monte Carlo (MC) simulation.

Instrumental $\not\!\!E_T$ is a result of energy mismeasurement in an otherwise $\not\!\!E_T$ balanced event. Instrumental $\not\!\!E_T$ sources in the $\gamma\gamma$ sample are separated into contributions from SM $\gamma\gamma$ events and events with at least one photon candidate originating from a misidentified jet (misID-jet), i.e., γ + jet and multijet events. The difference in energy resolution for real photons and fakes from misidentified jets results in a difference in the shape of the $\not\!\!E_T$ distribution between the two categories.

The $\not\!\!E_T$ shape in SM $\gamma\gamma$ events is modeled by using a dielectron (ee) data sample predominantly composed of $Z \to ee$ events. The ee sample satisfies the same kinematic requirements as the $\gamma\gamma$ sample, with the exception that the ee invariant mass is restricted to an interval about the Z boson peak to reduce genuine $\not\!\!E_T$ contributions (e.g., W + jet, diboson, and $t\bar{t}$ events). The $\not\!\!E_T$ distribution in ee events is compared with shapes in $Z \to ee$ and SM $\gamma\gamma$ MC events generated with PYTHIA [23]. These MC samples, and all others used in this Letter, were processed with full GEANT [24] detector simulation and standard reconstruction algorithms. Kinematic differences between the $Z \to ee$ and SM $\gamma\gamma$ processes are verified with MC to have a negligible impact on the $\not\!\!E_T$ shape. The $Z \to ee$ MC accurately models ee data for $\not\!\!E_T$ values below $\not\!\!E_T \approx$ 35 GeV. Above this value, a more pronounced tail is observed in ee data. The tail in data reflects both mismeasurements not modeled in MC and a small residual presence of genuine $\not\!\!E_T$ events in the ee sample. The average of the data and MC shapes is used to model the $\not\!\!E_T$ in SM $\gamma\gamma$ events for values of $\not\!\!E_T > 35$ GeV, and the data-only and MC-only extremes are used to define a systematic uncertainty on this shape.

The $\not\!\!E_T$ shape in misID-jet events is modeled with a data sample satisfying the same requirements as the $\gamma\gamma$ sample with the exception that at least one of the photon candidates fails the NN requirement. Additionally, photon identification requirements (iii) and (iv) are loosened to reduce the statistical uncertainty on the $\not\!\!E_T$ shape. A systematic uncertainty on the $\not\!\!E_T$ shape in events with misidentified jets is obtained by varying the photon identification criteria.

The instrumental $\not\!\!E_T$ background estimate is normalized such that the number of events with $\not\!\!E_T < 10$ GeV is equal to that in the $\gamma\gamma$ sample. The relative contribution of SM $\gamma\gamma$ and misID-jet background events is determined by a fit to the $\gamma\gamma$ sample $\not\!\!E_T$ distribution for $\not\!\!E_T < 20$ GeV. The fit accounts for the small contribution of SM background with genuine $\not\!\!E_T$ in the fit region and is verified to be insensitive to signal contributions for benchmark model cross sections relevant to this analysis. The SM $\gamma\gamma$ contribution to the $\gamma\gamma$ sample over the full $\not\!\!E_T$ range is $(41 \pm 17)\%$. A systematic uncertainty accounts for changes in the shape of the predicted instrumental $\not\!\!E_T$ distribution arising from the uncertainty in the determination of the SM $\gamma\gamma$ contribution.

SM background with genuine $\not\!\!E_T$ arises from real SM $\gamma\gamma + \not\!\!E_T + X$ events and from events with an electron misidentified as a photon (misID-ele.). The misID-ele. contribution is derived by using an $e\gamma$ data sample, composed primarily of instrumental $\not\!\!E_T$ sources for $\not\!\!E_T <$ 20 GeV and $W(\to e\nu)\gamma$ and $W(\to e\nu)$ + jet events at higher $\not\!\!E_T$ values. The instrumental $\not\!\!E_T$ sources are modeled with the previously introduced ee and misID-jet $\not\!\!E_T$ shapes, respectively. The $Z \to ee$ normalization is determined by fitting the Z boson peak in the $e\gamma$ invariant mass distribution, and the multijet $\not\!\!E_T$ shape is normalized to provide the remaining contribution in the $\not\!\!E_T < 10$ GeV region. The presence of real $\not\!\!E_T$ contributions in the $e\gamma$ sample is seen as an excess of events with high $\not\!\!E_T$ values above the predicted contributions from instrumental sources. This excess is well described by $W\gamma$ and W + jet events. The expected W boson peak is observed in the transverse mass distribution of $e\gamma$ sample events with $\not\!\!E_T > 30$ GeV. The normalization of the W + jet contribution is determined from a comparison of the data photon NN shape with MC real and fake photon NN shapes [19] in this $\not\!\!E_T$ region. The remaining contribution is in good agreement with PYTHIA $W\gamma$ production after applying a next-to-leading order (NLO) QCD correction [25] and an additional +15% scaling factor accounting for QED final state radiation in inclusive W production. The final state

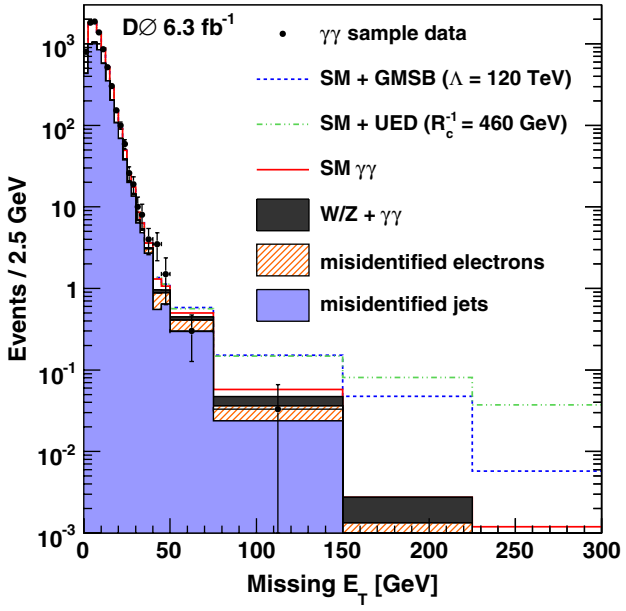

FIG. 1 (color online). $\not\!\!E_T$ distribution in the $\gamma\gamma$ sample shown with statistical uncertainty and expected SM background from events with a misidentified jet, a misidentified electron, $W/Z + \gamma\gamma$ events, and SM $\gamma\gamma$ events. The expected $\not\!\!E_T$ distribution in the presence of GMSB and UED events is also displayed for example values of Λ and R_c^{-1}, respectively.

TABLE I. Observed number of $\gamma\gamma$ events, predicted background from instrumental E_T sources (SM $\gamma\gamma$, γ + jet, QCD multijet) and genuine E_T sources ($W\gamma$, W + jet, $W/Z + \gamma\gamma$), and total predicted SM background, in three E_T intervals. The expected number of GMSB and UED signal events is listed for two Λ and R_c^{-1} values. The total uncertainty on the SM background and expected signal is given.

		SM background events			Expected signal events			
E_T interval (GeV)	Observed events	Instr. E_T	Genuine E_T	Total	GMSB $\Lambda = 100$ TeV	GMSB $\Lambda = 120$ TeV	UED $R_c^{-1} = 420$ GeV	UED $R_c^{-1} = 460$ GeV
35–50	18	9.6 ± 1.9	2.3 ± 0.5	11.9 ± 2.0	1.8 ± 0.1	0.3 ± 0.1	1.4 ± 0.1	0.3 ± 0.1
50–75	3	3.5 ± 0.8	1.5 ± 0.3	5.0 ± 0.9	4.1 ± 0.3	0.8 ± 0.1	2.9 ± 0.2	0.6 ± 0.1
>75	1	1.1 ± 0.4	0.8 ± 0.1	1.9 ± 0.4	14.3 ± 1.1	4.4 ± 0.4	24.7 ± 2.0	6.4 ± 0.5

radiation component [26] is determined with data using the $\Delta\mathcal{R}(e, \gamma)$ distribution. The predicted misID-ele. contribution to the $\gamma\gamma$ sample equals the excess of high E_T events in the $e\gamma$ sample, scaled by $f_{e\to\gamma}/(1 - f_{e\to\gamma})$, where $f_{e\to\gamma} = 0.020 \pm 0.005$ denotes the rate at which an electron fakes a photon satisfying the selection criteria, as measured with $Z \to ee$ data.

Real SM diphoton events with large genuine E_T originate from $W/Z + \gamma\gamma$ processes. This background contribution is estimated with MC by using MADGRAPH [27]. Events with inclusive W and Z boson decay modes are simulated, with $W \to l\nu(l = e, \mu, \tau)$ and $Z \to \nu\bar{\nu}$ providing the largest genuine E_T contribution. A total of 1.6 ± 0.1 $W + \gamma\gamma$ events and 3.8 ± 0.3 $Z + \gamma\gamma$ events are estimated to be present in the $\gamma\gamma$ sample. Figure 1 displays the $\gamma\gamma$ sample E_T distribution, which is in good agreement with the SM prediction over the full E_T range. Table I provides the observed number of $\gamma\gamma$ sample events and the SM prediction in three E_T regions.

We determine the sensitivity to the GMSB scenario by using a set of values, termed SPS8 [28], for the model parameters. In this set the scale Λ is unconstrained, $M_{\rm mes} = 2\Lambda$, $N_{\rm mes} = 1$, $\tan\beta = 15$, and $\mu > 0$ [28]. The masses and decay widths of SUSY particles are calculated with SUSYHIT 1.3 [29] and used to generate PYTHIA MC events. The event selection efficiency is 0.17 ± 0.02 at $\Lambda = 120$ TeV and does not differ significantly for other Λ values studied. The NLO production cross section is calculated with PROSPINO 2.1 [6]. The expected E_T distribution for the SM and GMSB at $\Lambda = 120$ TeV is depicted in Fig. 1. The number of expected GMSB events in three E_T regions is listed in Table I for $\Lambda = 100$ and 120 TeV.

We consider the UED model as implemented in PYTHIA 6.421 [30], leaving R_c^{-1} unconstrained and setting $\tilde{\Lambda}R_c = 20$, where $\tilde{\Lambda}$ is the cutoff scale for radiative corrections to KK masses. This UED model is implemented in a higher $(4 + N)$-dimensional space, where R_c^{-1} is much larger than that of the N compact extra dimensions accessible only to gravity, inducing KK particle decays through gravitational interactions. We choose $N = 6$ and a fundamental Planck scale $M_D = 5$ TeV, such that only the $\gamma^* \to G\gamma$ decay occurs with appreciable branching fraction [12]. The event selection efficiency is 0.19 ± 0.02 at $R_c^{-1} = 460$ GeV and

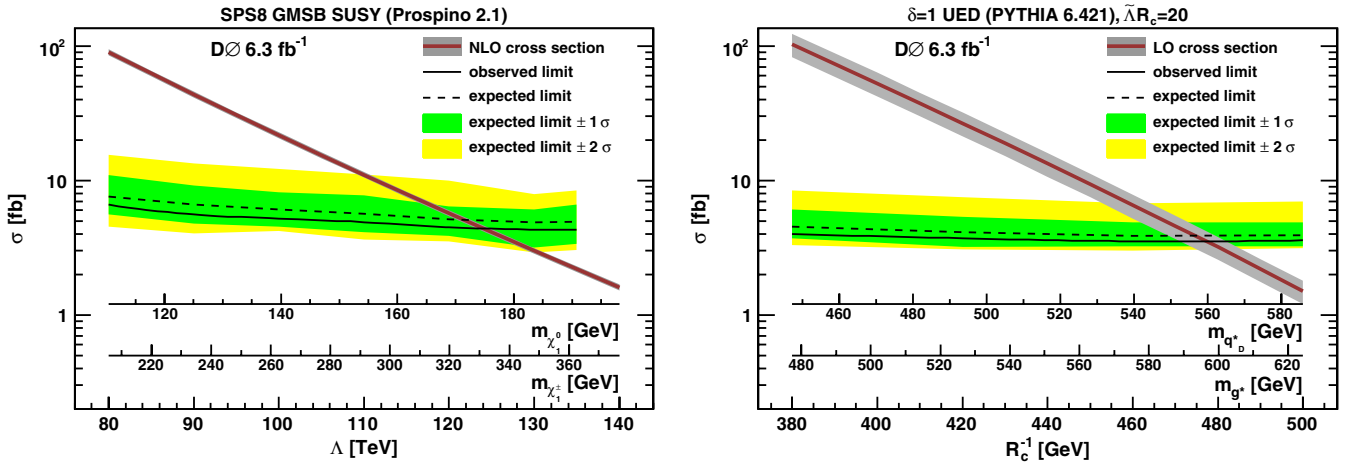

FIG. 2 (color online). The predicted cross section for the benchmark GMSB and UED models, and 95% C.L. expected and observed exclusion limits, as a function of Λ and R_c^{-1}, respectively. For the GMSB model, corresponding masses are shown for the lightest chargino $\chi_1^{\pm}$ and neutralino χ_1^0. For the UED model, corresponding masses are shown for the KK quark q_D^* and KK gluon g^*. The mass of the KK photon γ^* is approximately equal to R_c^{-1}.

does not differ significantly for other R_c^{-1} values studied. The expected $\not\!\!E_T$ distribution for the SM and UED at $R_c^{-1} = 460$ TeV is depicted in Fig. 1. The number of expected UED events in three $\not\!\!E_T$ regions is listed in Table I for $R_c^{-1} = 420$ and 460 GeV.

Systematic uncertainties for sources of instrumental $\not\!\!E_T$ are attributed to the uncertainty of the $\not\!\!E_T$ shape in SM $\gamma\gamma$ and misID-jet events and their relative normalization. An uncertainty in the shape of the $\not\!\!E_T$ distribution for the misID-ele. contribution arises from the uncertainty in the $Z \rightarrow ee$ contribution to the $e\gamma$ sample, and a 25% misID-ele. normalization uncertainty results from the $f_{e\rightarrow\gamma}$ uncertainty. Systematic uncertainties in the contributions estimated with MC arise from the integrated luminosity (6.1%), trigger efficiency (2%), and photon identification (3% per photon) and trajectory (3%) efficiencies. Uncertainty in parton distribution functions [31] yield systematic uncertainties of up to 5% and 20% in the production rate of GMSB and UED events, respectively.

No evidence for BSM physics is observed in the $\gamma\gamma$ sample $\not\!\!E_T$ distribution, and limits on the benchmark models are derived by using a Poisson log-likelihood ratio test [32] incorporating the full $\not\!\!E_T$ distribution. Pseudoexperiments are generated according to the background-only and signal plus background hypotheses and account for statistical uncertainty on the expected number of events and systematic uncertainties. The cross section limit is evaluated by using the CL_s modified frequentist approach [32]. Figure 2 shows the predicted GMSB and UED cross section with parton distribution function uncertainty and 95% C.L. cross section exclusion limit, as functions of Λ and R_c^{-1}, respectively. For GMSB, the NLO cross section uncertainty is small compared to the parton distribution function uncertainty. The UED NLO cross section has not yet been computed.

In conclusion, we have presented a search for physics beyond the standard model in the $\gamma\gamma + \not\!\!E_T + X$ final state at the Tevatron. The observed $\not\!\!E_T$ distribution is consistent with the SM expectation, and limits on two benchmark models are derived. In the SPS8 GMSB model, values of the effective SUSY breaking scale $\Lambda < 124$ TeV are excluded at 95% C.L. The limit excludes $m_{\chi_1^0} < 175$ GeV, representing improvements of 50 [18] and 26 GeV [16] with respect to previous measurements. Additionally, the first assessment is made of the sensitivity to the UED model with KK particle decays induced by gravitational interactions, excluding values of the compactification radius $R_c^{-1} < 477$ GeV at 95% C.L.

We thank the staffs at Fermilab and collaborating institutions and acknowledge support from the DOE and NSF (USA); CEA and CNRS/IN2P3 (France); FASI, Rosatom, and RFBR (Russia); CNPq, FAPERJ, FAPESP, and FUNDUNESP (Brazil); DAE and DST (India); Colciencias (Colombia); CONACyT (Mexico); KRF and KOSEF (Korea); CONICET and UBACyT (Argentina); FOM (The Netherlands); STFC and the Royal Society (United Kingdom); MSMT and GACR (Czech Republic); CRC Program and NSERC (Canada); BMBF and DFG (Germany); SFI (Ireland); The Swedish Research Council (Sweden); and CAS and CNSF (China).

[*]Visitor from Augustana College, Sioux Falls, SD, USA.
[†]Visitor from The University of Liverpool, Liverpool, United Kingdom.
[‡]Visitor from SLAC, Menlo Park, CA, USA.
[§]Visitor from ICREA/IFAE, Barcelona, Spain.
[‖]Visitor from Centro de Investigacion en Computacion—IPN, Mexico City, Mexico.
[¶]Visitor from ECFM, Universidad Autonoma de Sinaloa, Culiacán, Mexico.
[**]Visitor from Universität Bern, Bern, Switzerland.

[1] The variable $\not\!\!E_T$ is the magnitude of the vector in the plane transverse to the beam direction whose x and y components are $\not\!\!E_{T,k} = -\sum_i E^i_{T,k}$, with $k = x, y$, $E^i_{T,x} = E^i \sin\theta^i \cos\phi^i$, and $E^i_{T,y} = E^i \sin\theta^i \sin\phi^i$. The sum runs over all calorimeter cells measuring energy E^i, located at polar angle θ^i and azimuthal angle ϕ^i.
[2] M. Dine, A. E. Nelson, Phys. Rev. D **48**, 1277 (1993); M. Dine, A. E. Nelson, and Y. Shirman, Phys. Rev. D **51**, 1362 (1995); M. Dine *et al.*, Phys. Rev. D **53**, 2658 (1996); for a review, see G. F. Giudice and R. Rattazzi, Phys. Rep. **322**, 419 (1999).
[3] T. Applequist, H. C. Cheng, and B. A. Dobrescu, Phys. Rev. D **64**, 035002 (2001).
[4] S. Deser and B. Zumino, Phys. Rev. Lett. **38**, 1433 (1977).
[5] A. Salam and J. Strathdee, Nucl. Phys. **B87**, 85 (1975).
[6] W. Beenakker *et al.*, Phys. Rev. Lett. **83**, 3780 (1999).
[7] S. P. Martin, Phys. Rev. D **55**, 3177 (1997).
[8] P. Fayet, Phys. Lett. **70B**, 461 (1977); **86B**, 272 (1979); **175**, 471 (1986).
[9] S. Dimopoulos *et al.*, Phys. Rev. Lett. **76**, 3494 (1996); S. Ambrosanio *et al.*, Phys. Rev. Lett. **76**, 3498 (1996);K. S. Babu, C. Kolda, and F. Wilczek, Phys. Rev. Lett. **77**, 3070 (1996); H. Baer *et al.*, Phys. Rev. D **55**, 4463 (1997).
[10] C. Macesanu, C. D. McMullen, and S. Nandi, Phys. Rev. D **66**, 015009 (2002).
[11] T. G. Rizzo, Phys. Rev. D **64**, 095010 (2001).
[12] C. Macesanu *et al.*, Phys. Lett. B **546**, 253 (2002); C. Macesanu, Int. J. Mod. Phys. A **21**, 2259 (2006).
[13] A. Heister *et al.* (ALEPH Collaboration), Eur. Phys. J. C **28**, 1 (2003); J. Abdallah *et al.* (DELPHI Collaboration), Eur. Phys. J. C **38**, 395 (2005); P. Archard *et al.* (L3 Collaboration), Phys. Lett. B **587**, 16 (2004); G. Abbiendi *et al.* (OPAL Collaboration), Phys. Lett. B **602**, 167 (2004).
[14] B. Abbott *et al.* (D0 Collaboration), Phys. Rev. Lett. **80**, 442 (1998); F. Abe *et al.* (CDF Collaboration), Phys. Rev. D **59**, 092002 (1999).
[15] D. Acosta *et al.* (CDF Collaboration), Phys. Rev. D **71**, 031104 (2005).
[16] T. Aaltonen *et al.* (CDF Collaboration), Phys. Rev. Lett. **104**, 011801 (2010).

[17] V. M. Abazov *et al.* (D0 Collaboration), Phys. Rev. Lett. **94**, 041801 (2005).
[18] V. M. Abazov *et al.* (D0 Collaboration), Phys. Lett. B **659**, 856 (2008).
[19] V. M. Abazov *et al.* (D0 Collaboration), Phys. Lett. B **690**, 108 (2010).
[20] V. M. Abazov *et al.* (D0 Collaboration), Nucl. Instrum. Methods Phys. Res., Sect. A **565**, 463 (2006).
[21] T. Andeen *et al.*, Report No. FERMILAB-TM-2365, 2007.
[22] G. C. Blazey *et al.*, arXiv:hep-ex/0005012.
[23] T. Sjöstrand *et al.*, Comput. Phys. Commun. **135**, 238 (2001).
[24] R. Brun and F. Carminati, CERN Program Library Long Writeup No. W5013, 1993 (unpublished).
[25] U. Baur, T. Han, and J. Ohnemus, Phys. Rev. D **48**, 5140 (1993).
[26] J. Cortes *et al.* Nucl. Phys. **B278**, 26 (1986).
[27] J. Alwall *et al.*, J. High Energy Phys. 09 (2007) 028.
[28] B. C. Allanach *et al.*, Eur. Phys. J. C **25**, 113 (2002).
[29] M. M. Mühlleitner *et al.*, Acta Phys. Pol. B **38**, 635 (2007).
[30] M. ElKacimi *et al.*, Comput. Phys. Commun. **181**, 122 (2010).
[31] J. Pumplin *et al.*, J. High Energy Phys. 07 (2002) 012; D. Stump *et al.*, J. High Energy Phys. 10 (2003) 046.
[32] T. Junk, Nucl. Instrum. Methods Phys. Res., Sect. A **434**, 435 (1999); W. Fisher, Report No. FERMILAB-TM-2386-E, 2006.